In-depth investigation of a third body formed by selective transfer in a NiCr / AgPd electrical contact

Manon Isard, Imène Lahouij, Jean-Michel Lanot, Pierre Montmitonnet

Version of Record: https://www.sciencedirect.com/science/article/pii/S0043164821001423
Manuscript_4f1f4fc9f37015e6fcaa3a9a0b6b2cb1

In-depth investigation of a third body formed by selective transfer in a NiCr / AgPd electrical contact

Manon Isard[1,2], Imène Lahouij[1], Jean-Michel Lanot[2] and Pierre Montmitonnet[1]
1. MINES ParisTech, PSL Research University – CEMEF, Centre de Mise en Forme des Matériaux, CNRS UMR7635, Sophia Antipolis, France
2. Vishay S.A, Nice, France

Abstract

The aim of this work is to investigate the physical and chemical mechanisms involved in the formation process of a third body in an electrical contact. The device studied is an electric rheostat position sensor consisting of a low pressure sliding contact between a resistive body (NiCr) and a contactor (AgPd). The contact is lubricated with a silicone oil / PTFE grease and operating under boundary lubrication condition. It was previously shown that the degradation of the electrical behavior of the contact is mainly due to a severe abrasive wear of the NiCr surfaces, enhanced by the formation on the AgPd contactor of a hard and adhesive transfer enriched in Nickel (Ni). In the current work, In-depth cross-section analyses combining focused ion beam (FIB) with analytical transmission electron microscopy (TEM) techniques are used to identify the structural and chemical changes that undergo by the interfacial contact involving NiCr and AgPd surfaces. The results highlight a selective character (Ni alone transferred from NiCr alloy) and a nanocrystalline structure of the Ni third body adhering to the noble counterpart. Several hypotheses involving severe plastic deformation (SPD) of the NiCr surface, catalytic effect of Pd element and/or Cr salts volatility are discussed. Furthermore, it was found that the deposition of alumina powder on the NiCr surface using a tumble finishing treatment inhibits the formation of the detrimental third body, which preserves the contact from severe wear and leads to a significant improvement of the electrical behavior of the position sensor. The role of alumina in preventing the contact from wear is discussed and a scenario explaining the evolution of the interfacial contact at operating conditions is proposed.

Keywords: tribological interface, wear, third body, solid lubricant, transmission electron microscopy

1. Introduction

Tribological interfaces consisting of a contact between two bodies operating under boundary-lubricated sliding conditions are subjected to irreversible transformations which result from physicochemical and mechanical surface interactions. These transformations give rise to a new surface material called ‘third body’ which exhibits in most cases completely different friction and wear properties compared to the original contact. The formation of the third body involves numerous synergetic effects such as wear of surfaces, material transfer, formation of micro-cracks, phase transformations, deformation hardening, formation of oxides, and reaction with lubricant additives. [1]
Wear is considered as a phenomenon playing a major role in the formation process of a third body through the detachment of debris from the rubbing surfaces and their compaction in the contact [2]. The material characteristics of the rubbing surfaces and the operating conditions of the contact are found to have an impact on the size of the wear debris. Moreover, once formed, wear debris can undergo changes in terms of size, morphology and composition

which impact their mechanical properties. Godet [2] states that during a fretting test, wear debris detached from steel surfaces have been transformed first into magnetite and then into hematite, which behave differently when trapped in a contact. More generally, it is admitted that for metallic materials, the corresponding nano-sized debris are usually harder than the rubbing surfaces, therefore, they could give rise to a third body that promotes wear.
On the other hand, friction between metallic sliding surfaces is known to produce ultrafine-grained layers, via Severe Plastic Deformation (SPD) [3-7] giving rise to Tribologically Transformed Surfaces (TTS) [8, 9]. These layers are confined to the region just below the wear surface. It was found that the evolution of these subsurface layers involves the formation of steep dislocation gradients and cell walls, as well as processes such as grain refinement and dynamic recovery.
Moshkovich et al. [10] investigated the behavior of FCC metals such as Ag, Cu, Ni, and Al under lubricated conditions. They found that friction and wear properties in the boundary lubrication region are characterized by the formation of a nanocrystalline structure associated to deformation hardening and dynamic recovery, but not with a formation of tribofilms as usually observed with different additives to pure oil. A direct correlation was observed between the wear coefficient and parameters such as the steady-state hardness/stress, the stacking fault energy (SFE) and the melting temperature. The authors highlighted that increasing these parameters leads to decreasing the wear coefficient.
Popov et al. [11] investigated the evolution of the microstructure and nano-hardness of Ag and Ni metals after friction in boundary lubrication regime. Through plastic deformation induced by sliding, gradients of grain size and hardness with depth were revealed respectively by TEM imaging and nanoindentation. It was shown that deformation twinning followed by limited recovery within the superficial layer of Ag led to the formation of a relatively thick subsurface layer of ultra-fine equiaxed grains. During the friction of Ni, thermally activated processes for the rearrangement and annihilation of dislocations are accelerated due to its high SFE and contact temperature. Moreover, nanoindentation results highlighted that the hardening increases with SFE under friction in lubricated conditions, therefore the best wear properties observed for Ni in comparison to Ag were related to higher hardening due to its higher SFE. Hence, microstructural evolutions that surfaces undergo under boundary lubrication regime could impact the friction and wear behavior of contacts in different ways. In some instances, the tribologically induced surface layers can result in an evolution towards low-wear behavior while in others, the hardening of the near surface layers can promote either abrasive wear of the softer counterpart, or lead to the formation of a third body composed by hardened nanoparticles in the contact, oxidized or not [11]. Under such conditions, even the nominally harder of two bodies in contact can undergo abrasion.

Wear and third body formation have a major impact on the lifetime of electric contacts as well as on the electrical signal quality [12, 13] ; this is particularly troublesome where high precision is required for very long times. In our previous work [14] we have shown a direct correlation between degradation of the electrical properties of sensors and severe abrasive wear of NiCr surface track in contact with AgPd cursor. The paradoxical wear undergone by the Ni-based superalloy (430 Hv) in contact with the AgPd noble alloy (270 Hv) was attributed to the formation of a patchy layer rich in Ni on the AgPd surface. A tumble finishing treatment using alumina powder was found to improve the electrical behavior of the sensors. It has been shown that this improvement is related to the role of alumina particles to reduce wear and stop the growth of the Ni transfer layer. However, a definitive understanding of both the formation mechanisms of the Ni transfer layer and the role of Alumina in delaying the Ni transfer is still not well established. The present work provides detailed in-depth characterizations of the contact interfaces, especially of structural and chemical properties via in-depth cross-section examination combining focused ion beam (FIB) with analytical

transmission electron microscopy (TEM) techniques. The aim is to understand the physical mechanisms that take place at the AgPd-NiCr electrical contacts in order to improve their durability.

2. Electrical components

The electrical component investigated in this study is a position sensor developed for aeronautical applications. The triboelectric contact inside the sensor is composed of:
- a resistive track made out of a Ni-based alloy (NiCr) with a periodic geometry (Figure 1); this particular Ni-based alloy is selected for its stable electrical resistivity when temperature changes.
- a sliding cursor made out of an AgPd alloy, sliding on the track to collect an electrical tension (the applied electrical current is 1 mA, i.e. ~3 $A.mm^{-2}$). The electrical contact is ensured between the curved cursor and track "plateaus" (Figure 1), whereas track "valleys" are used as lubricant reservoir and wear particles trap. The nominal contact stress is around 5 MPa.

The 5 µm thick NiCr foil has been hardened by a long cold rolling schedule. The AgPd alloy has gone through an aging heat treatment to be given a higher hardness and more wear resistance. The nominal hardness values of the used NiCr and AgPd materials are respectively 430 Hv and 270 Hv.

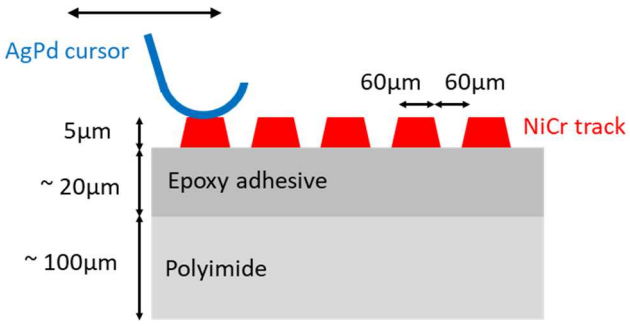

Figure 1: Contact geometry inside the sensor composed by an AgPd cursor in contact with NiCr track. Only a cross section of the coil-shaped NiCr track is shown. [14]

The lubricant is a chlorinated silicone oil, PTFE-thickened grease deposited manually on the track during the manufacturing process. PTFE is present as microspheres of ~ 2 µm in diameter. This lubricant has been used for a long time in electrical contacts because of its chemical inertness, low volatility and stable viscosity over a wide range of temperatures, and high resistance to arcing. It ensures a boundary regime of lubrication, mandatory to keep a sufficient number of direct metal-metal contact spots to keep good electrical contact.

3. Experimental Methods

3.1. Endurance tests

An endurance test consisting in ca. 3.5 million cycles of back and forth linear movements is applied on all finished parts. The test has been elaborated to reproduce real movements impacting parts during their lifetime, alternating low amplitude vibrations (~ 3 mm / 1 Hz) and large amplitude actuations (~ 15 mm / 0,3 Hz) ; the corresponding average sliding velocities are 6 and 10 $mm.s^{-1}$.

3.2. Tumble finishing treatment

To improve the contact surfaces, tumble finishing has been applied on some NiCr surfaces. It consists in introducing glass balls, distilled water and alumina powder in a rotating barrel, with the tracks glued on its wall. The alumina powder is composed of lamellar particles of 10 nm to 1 µm in size, with a thickness of about 50 nm [14].

3.3. Analytical tools

All samples have been observed and analyzed with Scanning Electron Microscope (SEM) (Zeiss Supra 40), using the Secondary Electron (SE) mode when topography is to be enhanced and the Backscattered Electrons (BSE) mode when chemical contrast is to be enhanced. SEM observations have been coupled with Energy Dispersive X-Ray Spectroscopy (EDS) (Quantax QX400). The EDS analyses were carried out using beam energy of 15 keV corresponding to an analysis depth of approximately 1 µm.
The microstructure of NiCr tracks has been observed in SEM as follows:

- SEM observations by the surface, after electrolytic polishing using Kalling's solution (58,6%wt HCl, 38,9%wt ethanol and 2,5%wt $CuCl_2$). The etching step is followed by polishing with silica nanoparticles during 4 hours;
- SEM observations in cross section, after a transversal ion polishing (6 kV during 8 hours) performed from the polyimide substrate;
- Electron Back-Scattered Diffraction (EBSD) analyses were conducted to analyze the grain structure and the surface texture of the NiCr track.

TEM cross-sectional samples on NiCr and AgPd surfaces were prepared using TESCAN Lyra3 FIB-SEM instrument Focused ion Beam (FIB) technique. A transversal cut was performed on the worn surface to obtain a 100 nm thick cross section. Platinum layers were previously deposited on surfaces to preserve them from nanomachining by Ga+ ion beam.
TEM observations were performed on a JEOL 2100F field emission gun operating with 200 KV accelerating voltage equipped with Energy Dispersive Spectroscopy (EDS) and equipped with GATAN Imaging Filter (GIF200). Different imaging modes have been used:

- Scanning Transmission Electron Microscopy (STEM) gives similar images to SEM but in a much smaller interaction volume;
- Bright Field (BF) and Dark Field (DF) modes provide different contrasts and allow observing more details in the microstructure;
- Selected Area Electron Diffraction (SAED) informs about the crystalline state.

4. Evolution of the AgPd-NiCr contact under endurance tests without Al_2O_3 tumble finishing treatment

4.1 Relationship between electrical response of the contact and wear under endurance tests

Table 1 displays three typical cases resulting from endurance tests applied to the position sensors. The first one concerns the so-called 'Passed endurance tests' characterized by a resistance drift recorded at the end of the test lower than 1%, the acceptability threshold, and low wear of the NiCr tracks. The second case illustrates the so-called 'Failed endurance tests' characterized by a high resistance drift (larger than the threshold 1%) and a severe wear of the NiCr tracks. SEM analyses carried out on AgPd and NiCr surfaces as shown in [14] have given evidence of the presence of an adherent transfer layer on the surface of the AgPd cursor. EDX analysis shows that it is composed almost exclusively of nickel whereas the alloy initially contains ~20% Cr.

As detailed previously in [14], these observations have confirmed the existence of a direct correlation between the transfer layer formation on AgPd surface and excessive resistance drift of the sensors: the higher the resistance drift, the more abundant the transfer of material on the AgPd surface. This correlation suggests that the transfer layer contributes to the severe abrasion of the NiCr tracks.
Hence, in order to improve the protection of the contact surfaces against wear, an alumina assisted tumble finishing treatment was applied to the NiCr surfaces. The barrel tumble finishing treatment has been used to deburr aggressive surface edges of NiCr tracks, suspected to be involved in initiating the severe wear observed after endurance tests.
Thanks to this treatment, considerable improvement of the electrical endurance of the sensors was observed in terms of value of drift and percentage of 'passed test'. In order to better understand the formation mechanisms of the transfer layer on the AgPd cursor and its role in damaging the electrical response of sensors, and the role of alumina in enhancing the electrical behavior of sensors when the tumble finishing treatment is applied, we focus in the following on the characterization of the AgPd-NiCr contact surfaces before and after endurance tests.

Sensors	**Resistance drift**	**NiCr track surface**	**AgPd cursor surface**
AgPd-NiCr contact without tumble finishing (passed endurance test)	Low drift 64 Ω (= 0,64%)	Low wear Material loss ~0,85%	Mild abrasive wear
AgPd-NiCr contact without tumble finishing (failed endurance test)	High drift 257 Ω (= 2,57%)	Severe abrasive wear Material loss ~ 2,50% **(TEM cross-section 1)**	Transfer layer rich in Ni **(TEM cross-section 2)**
AgPd-NiCr contact with tumble finishing (passed endurance test)	Low drift < 40 Ω (= 0,40%)	Low wear (not measurable) **(TEM cross-section 3)**	Severe abrasive wear

Table 1: Relationship between wear and electrical resistance for AgPd-NiCr contacts with and without the tumble finishing treatment. Resistance drift values were recorded at the end of endurance tests carried out on sensors. The position sensor is rejected if the resistance drift is higher than 1% (threshold value). The consequence of the resistance drift is an offset between the real and the transmitted position-resistance relation. The percentage of material loss was estimated from profilometry measurements on an area of 1 mm x 1 mm on the NiCr tracks. AgPd and NiCr surfaces were observed in SEM after endurances tests. Further details regarding the measurements of resistance drift and wear loss are available in [14]

4.2 Characterization of the virgin NiCr surface before endurance tests

Figures 2a and 2b present respectively SEM-BSE observations of the NiCr track on the top surface and on the cross-section obtained by ion polishing.
The NiCr grains are typical of cold rolled samples: they are elongated, with an average thickness of 500 nm, an average width of 10 µm and an average length of 200 µm. Therefore, the most probable estimation of elongation factor is between 15 and 20 after the last recrystallization step in the foil rolling process. SEM-BSE images show grey level contrasts, but EDS analyses (confirmed by XPS) prove that the NiCr surface has a homogeneous chemical composition at the μm^3 scale, close to the nominal Ni:Cr ratio of 80:20. The grey level contrast is therefore attributed to a minor effect of crystallographic orientation of the BSE detector. The NiCr material is chemically homogeneous as verified with EDS analyses; it did not contain second phase or precipitates. The two thin and white layers visible on the top and bottom of the cross section are attributed to transversal ion polishing which leads to a non-perfectly plane surface.

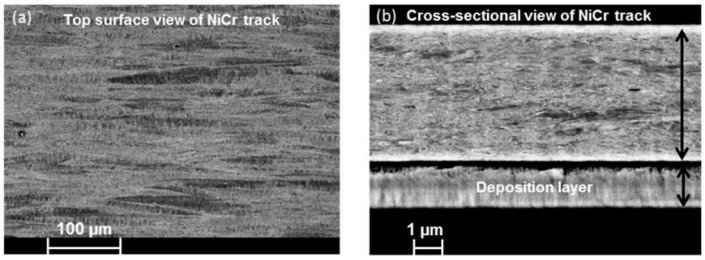

Figure 2: SEM-BSE images of NiCr track; (a) image taken on the top surface of NiCr track and (b) image of the cross section of the NiCr track, where the thickness of 5 µm is apparent, covered by a re-deposition layer due to the transversal ion polishing process. The two thin white layers on the top and bottom of NiCr cross section are attributed to the sample preparation (which leads to a non-plane, slightly cambered surface).

Figure 3 displays EBSD analysis carried out on the top surface of the NiCr track. Using the Ni CFC structure (a = 3.571 nm), 90% of the pixels were indexed. The map shows different colors in the same grain; most grains are oriented in the [101] direction, but some defects are oriented in the [111] direction, which is imputed to micro-shear bands caused by the cold rolling process. More generally, the NiCr microstructure seems to have undergone severe deformation, which results in heterogeneous crystallographic orientation even in the same grain.

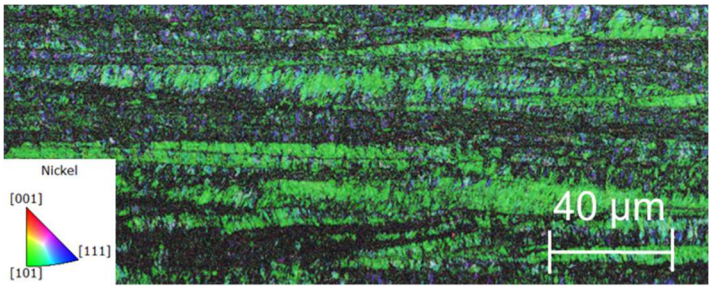

Figure 3: EBSD map showing the elongated NiCr grains ; analysis carried out on the top surface of NiCr track.

4.2 TEM analyses of the NiCr track after endurance tests

A TEM lamella was extracted from the worn surface of the NiCr track after the failed endurance test described in table 1 (cross-section 1). The location of the lamella is shown in Figure 4.

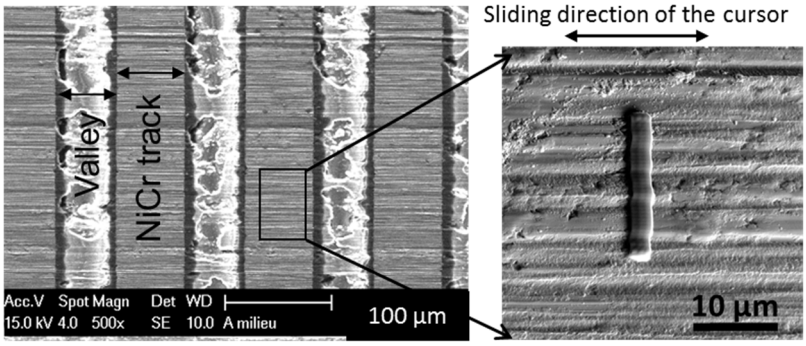

Figure 4: Location of the TEM lamella extracted in the worn surface of the NiCr track after a failed endurance test (TEM cross section 1). The test result descriptions are detailed in table 1.

The STEM micrograph of the NiCr lamella (Figure 5) is representative of the entire TEM examination of the cross-sectional lamella. As can been seen, reciprocating sliding movements of the AgPd cursor on the NiCr track result in SPD phenomena of the subsurface within a depth of approximately 580 nm. Despite the moderate conditions of the endurance

tests (lubricated contact and applied pressure of 5 MPa), the deformed layer reaches a thickness corresponding to 10% of the total thickness of the 5 µm-NiCr track, which attests severe damage experienced by the track during the endurance test.
The near-surface material (depth ~ 600 nm) is crystalline and made of equiaxed, fine grains, while the subsurface bulk material (depth > 600 nm) consists of elongated grains similar to the ones observed by SEM and EBSD. This is generally found after SPD.

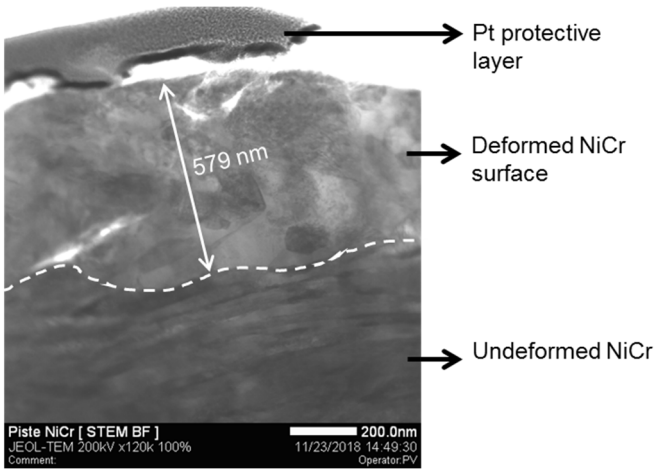

Figure 5: STEM-BF image of the cross-section of NiCr track after the failed endurance test (TEM cross section 1) showing three different layers: the platinum layer deposited prior to the milling process, a highly deformed layer and the bulk NiCr layer.

On some areas of the top surface of the same lamella, a kind of compacted nanocrystalline grains embedded into the NiCr substrate is observed as can been seen in Figure 6a and 6b (area highlighted with red line). These areas have nanocrystalline structure, which is illustrated with the SAED analyses. The diffraction pattern of the un-deformed NiCr material shows discrete diffraction spots (Figure 6c), whereas for the inlaid area, the diffraction pattern is organized in rings which reflect a large number of randomly oriented grains present in a small diffraction volume (Figure 6d), specific of nanocrystalline structure.

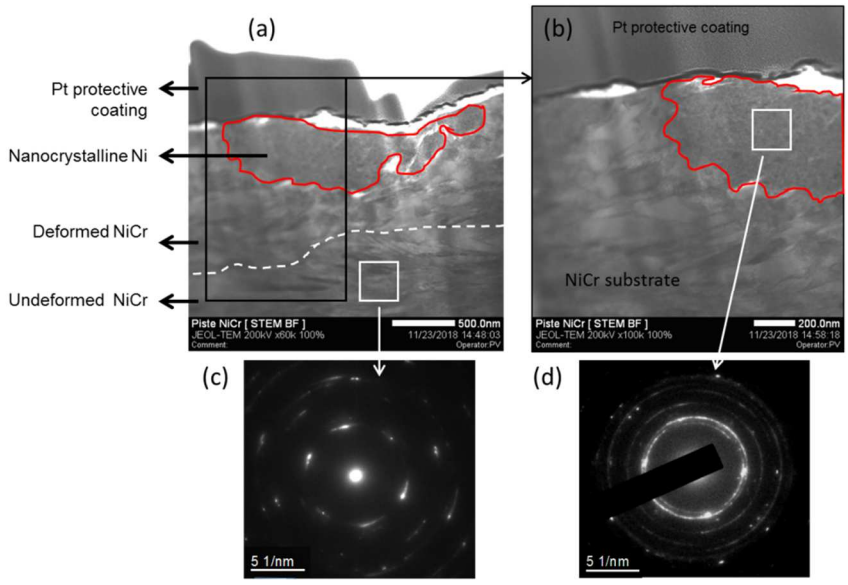

Figure 6: (a) STEM-BF image of the TEM cross-section 1 of the NiCr track after a failed endurance test showing three areas: undeformed NiCr, deformed NiCr and an inlaid nanocrystalline layer. (b) A zoom in of (a) showing the inlaid nanocrystalline layer. (c) SAED pattern of the non-deformed NiCr substrate with well-defined diffraction direction. (d) SAED pattern of the inlaid layer organized in rings.

The EDS analyses carried out on the NiCr cross-section show that the inlaid layer is mainly composed of pure Ni. EDS elemental mappings of Cr and Ni elements displayed in Figure 7 confirms the absence of Cr in the inlaid layer, whereas the NiCr substrate contains both Ni and Cr elements with a ratio close to the initial ratio 80/20.
Hence, TEM and EDS analyses give evidence that the NiCr tracks after failed endurance tests are subjected to severe plastic deformation and abrasive wear. Moreover, the presence in some areas of the TEM cross section of layers composed of compacted nanocrystalline Ni embedded into the NiCr surface need to be clarified especially regarding their role in causing the damage of the NiCr track, and therefore the failure of the electrical behavior of the sensors. To this end, the corresponding AgPd cursor used to slide against the NiCr track was investigated in the same way by TEM.

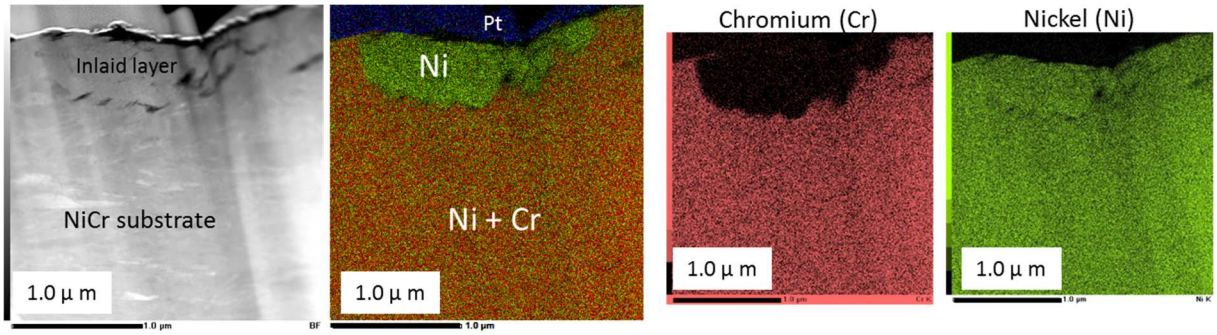

Figure 7: STEM micrograph of NiCr cross section lamella and its corresponding EDS mapping.

4.3 TEM analyses of AgPd cursor after endurance test (cross-section 2)

Figure 8 shows three different steps of the FIB cross section machining carried out on the AgPd cursor used to slide against the NiCr analyzed in section 4.2. The cursor was subjected to the failed endurance test described in table 1.

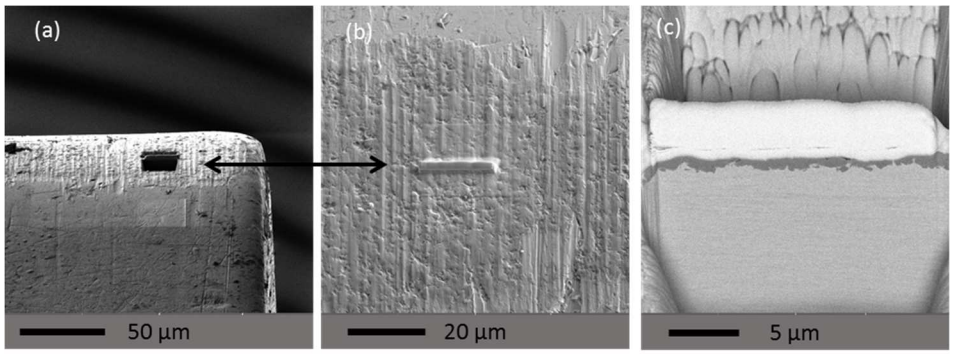

Figure 8: SEM images carried out during the FIB sectioning of a TEM lamella from the AgPd cursor. (a) shows the location of the TEM lamella; (b) shows a zoom in of the contact area and (c) shows the cross section prior to the lift out where a contrasted thick layer is visible between the platinum protective coating and the AgPd substrate.

As can be seen in Figure 9a, the TEM low magnification cross section of the AgPd cursor reveals that the AgPd surface was subjected to severe plastic deformation through a depth of about 500 nm. Moreover, the formation of a third body of a thickness of ~1 µm is confirmed. The interface between the AgPd surface and the third body is not sharp, attesting severe deformation prior to the formation of the third body. Higher magnification observation displayed in Figure 9b highlights the nanocrystalline structure of the third body which seems to be composed of compacted nanoparticles. SAED pattern carried out on the third body is organized in continuous rings, which confirms its nanocrystalline structure.

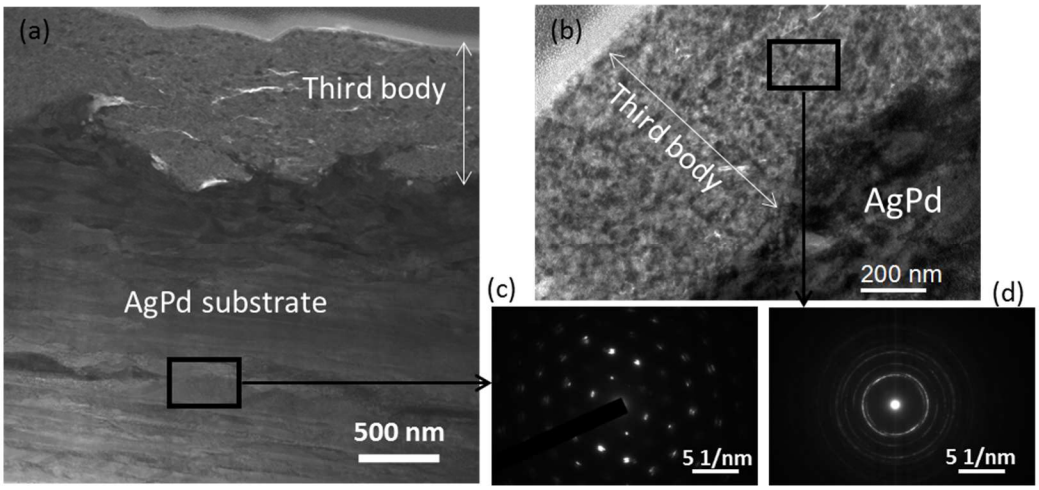

Figure 9: TEM-BF image of the AgPd cursor, covered by the third body; (a) the third body layer is about 1 µm thick; (b) Zoomed area of (a) where it is possible to see a specific nanostructure, similar to embedded nanoparticles. (c) and (d) SAED patterns carried out respectively on AgPd substrate and third body.

EDS results displayed in Figure 10 show that the third body is mostly composed of Ni, while small amounts of Ag and Pd are detected (Cr is almost absent). Hence, the third body formed on the AgPd surface is selective in Ni. The AgPd wear debris seems to be preferentially mixed within the grease. Their presence in the contact does not seem to cause surface damage.

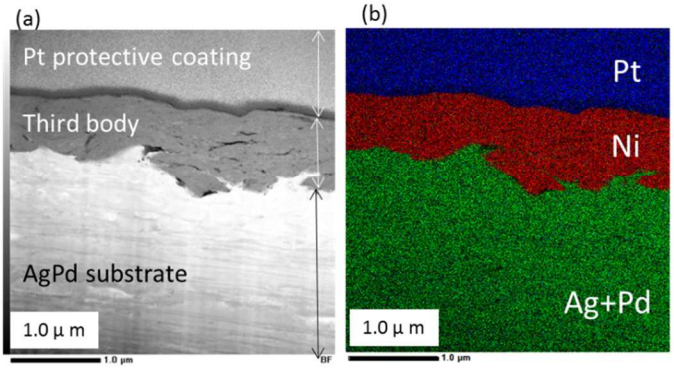

(c)

Elements	AgPd substrate (%at)	Third-body (%at)
O	2	3
Ag	47.5	2.8
Pd	49.3	2.9
Cr	0,2	0.3
Ni	1	91

Figure 10: (a) STEM-BF micrograph of the AgPd cross section showing the presence of a third body, (b) the corresponding EDS mapping showing that the third body is mainly composed of Ni, (c) table displaying the atomic composition of the AgPd substrate and the third body

As discussed later in section 6, the nanostructured third body is hard enough to cause severe wear of tracks, but brittle enough that in some cases, Ni fragments detached from the third body adhering to the AgPd cursor are back-transferred into the NiCr tracks. This points to the dynamic and reversible character of the formation mechanism of adhesive transfers [15,16]. Therefore, improving the wear behavior of the contacts requires a solution to avoid the formation of this aggressive third body.

5. Role of the tumble finishing in improving the endurance of sensors

To limit the formation of the aggressive third body, an effective treatment has been found through barrel tumble finishing of NiCr tracks with glass beads and alumina powder. It has been introduced in the process initially to deburr sharp surface edges to improve the wear resistance of surfaces [17].

5.1 Impact of the tumble finishing treatment on the NiCr surfaces

In order to analyze the impact of the tumble finishing treatment on the surface of the NiCr track, in particular the role of alumina powder, tumble finishing treatments with and without alumina powder were applied to the NiCr surfaces. As can be seen in Figure 11a and 11b, the tumble finishing treatment containing only the glass beads and distilled water leads to a smoothing of the top surface of NiCr. However, the roughness and surface irregularities of the edges are intensified (Figure 11b and 11b'). Adding alumina powder to the tumble finishing treatment improves the deburring of the edges; the surface irregularities are filled with alumina. Moreover, the top surfaces are found to be covered by a layer of alumina powder (Figure 11c and 11c'), as described in more details in a previous study [14].

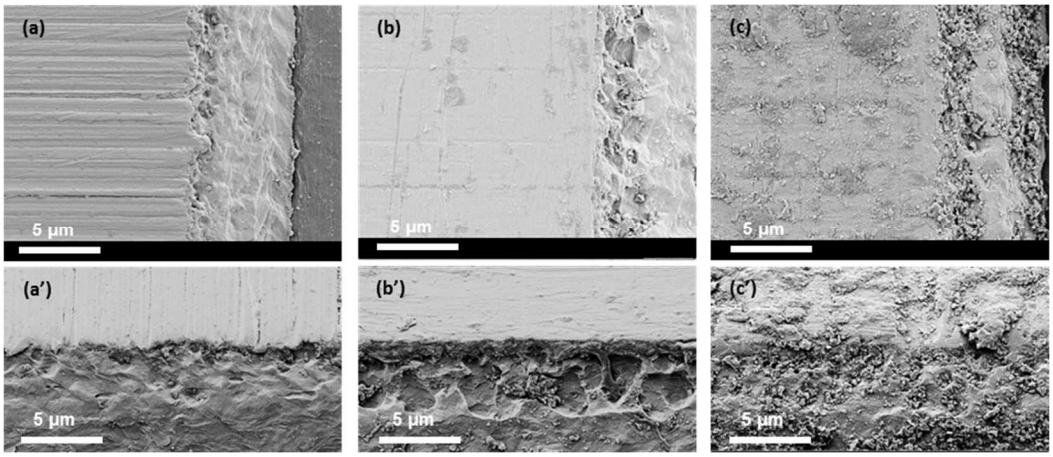

Figure 11: SEM-SE observations of NiCr tracks focused on the edges; (a) and (a') surface without tumble finishing tilted respectively at 0° and 40°; (b) and (b') surface treated by tumble finishing without alumina powder tilted respectively at 0° and 40°; (c) and (c') surface treated by tumble finishing with alumina powder tilted respectively at 0° and 40°.

5.2. Impact of the tumble finishing treatment on the electrical behavior of sensors

All the endurance tests carried out with treated NiCr tracks show a significant improvement of the resistance drift. While 90% of the endurance tests carried out with sensors equipped with non-treated tracks gave a resistance drift higher than 60 Ω, 100% of sensors equipped with treated NiCr tracks give a resistance drift lower than 60 Ω (Figure 12).

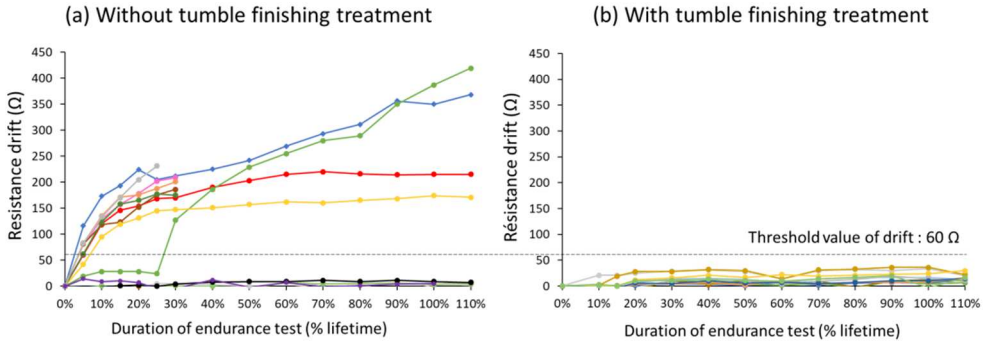

Figure 12: Improvement of electrical properties of sensors due to tumble finishing. (a) Resistance drift profiles of sensors without treatment; (b) Resistance drift profiles of sensors with tumble finishing treatment. Campaign of tests carried out on about 50 sensors. On the horizontal axis, 100% represents 3.5 10^6 cycles.

5.3. Impact of the tumble finishing treatment on the wear behavior of the AgPd-NiCr contact during endurance test (TEM cross-section 3)

In order to better understand the role of the tumble finishing treatment in improving the electrical behavior of sensors, a TEM lamella was extracted from the worn surface of the NiCr track after an endurance test described in table 1 (cross-section 3). The location of the lamella is shown in Figure 13.

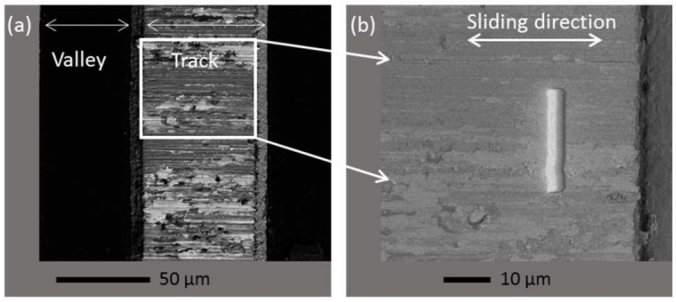

Figure 13: SEM images carried out during the FIB sectioning of a TEM lamella from the treated NiCr track showing the location of the cut.

Figure 14 shows an overview of the cross-section of the treated NiCr track after an endurance test. The overall grain morphology of the material of the track is characterized by an elongated shape similar to the ones observed on the raw NiCr material (Figures 2 and 3), which indicates the absence of any deformation and/or damage of the microstructure. However, the near-surface (a layer of ~100 nm thickness) is different in comparaison with the rest of the material. It appears less contrasted in the TEM image and exhibits some degree of grain refinement which indicates that the near-surface experienced a moderate plastic deformation during the endurance test.

On the other hand, the comparison with the TEM cross section of untreated NiCr track displayed in Figures 5 and 6 highlights the role of alumina in preventing the NiCr surface from high plastic deformation and severe wear by acting as a solid lubricant.

Indeed, neither severe damage, nor inlaid wear nanoparticles are observed on the top of the treated NiCr surface.

However, higher maginification observation of the top surface shows the presence of a thin transfer of a few tens of nanometers of thickness (Figure 15a and 15b). EDS mapping reveals that this transfer layer is mainly composed of Ag and Pd elements which indicates that a transfer of AgPd wear debris on the NiCr surfaces is taking place during the endurance test. As shown in Figure 15a, this transfer is not covering the whole NiCr surface and has a limited thickness. Hence, it does not lead to a deterioration of the electrical signal.

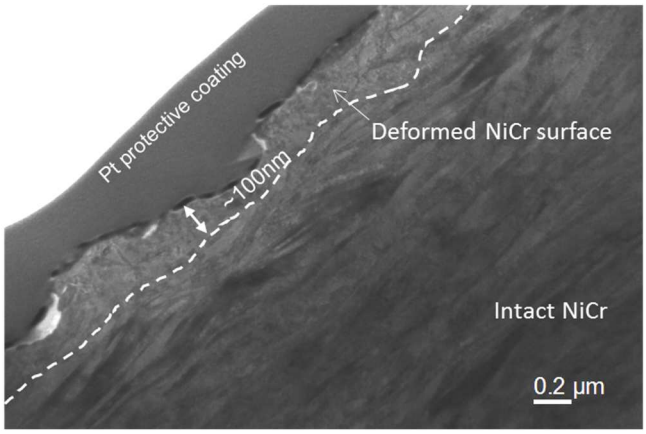

Figure 14: TEM-BF image of the NiCr track treated with alumina tumble finishing after an endurance test (TEM cross section 3). The first 100 nm of the surface are subjected to plastic deformation.

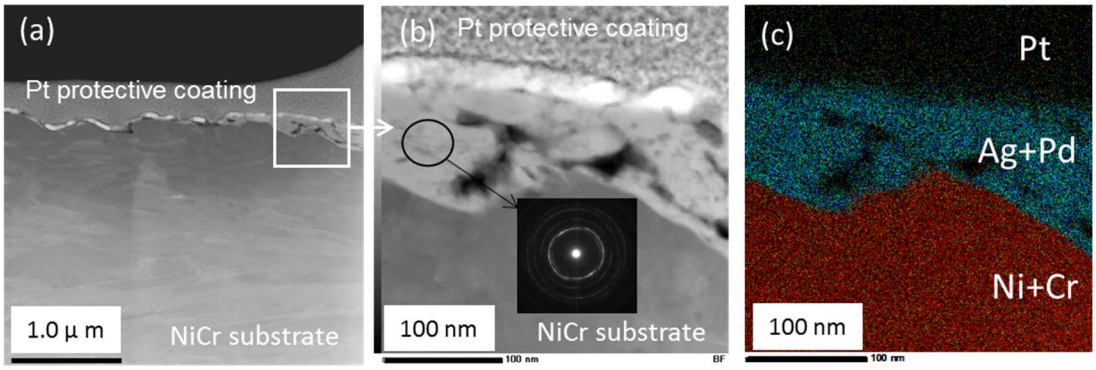

Figure 15: (a) STEM-BF micrograph of the treated NiCr cross section 3 showing the presence of a transfer with an average thickness of 100 nm; (b) STEM-BF image of a zoomed area from (a) and SAED pattern of the transfer layer; (c) the corresponding EDS of micrograph (b).

The structure of the transferred AgPd layer in comparison with the bulk AgPd material is provided by TEM-SAED analyses (Figure 9c and 15a). The SAED pattern obtained from the bulk AgPd shows discrete diffraction spots, whereas the transferred AgPd layer shows continous ring pattern built up by many grains, necessarily extremely small, which suggests a nanocrystalline structure.

6. Discussion

This study was undertaken with two objectives:

- to understand the formation mechanisms of the adhesive and selective Ni third body generated in an electrical sliding contact of AgPd cursor on NiCr track;
- and to explain the beneficial effects of the tumble finishing treatment in preventing surfaces from severe wear and third body formation.

Some hypotheses have been previously discussed [14], but the current work based on TEM observations gives further details.

6.1 Nanostructured adhesive transfer layer formation and abrasion of the nominally harder body by the nominally softer one

It is admitted that cyclic sliding movements can give rise to a change of the microstructure of the near-surface materials resulting from high plastic deformation experienced by the contact, forming Tribologically Transformed Layers (TTL). In the case of the AgPd-NiCr contact which is operating under boundary lubrication, sliding movements were found to lead to a grain refinement of the NiCr material from elongated 200 x 10 x 0.6 µm grains down to a size in the range of 10-50 nm with an intermediate zone with grains ~100 nm (figure 5). Such nanocrystalline layer is found in the mild wear case ('passed endurance test', illustrated here with Al_2O_3-enhanced tumble finishing, figure 14) as well as in the severe wear case with deep scratches ('failed endurance test'). The TTL is deeper and finer grained in the latter case. The grain refinement is found to be associated with changes in friction and wear behavior of metals. Argibay et al. [18] have proposed a model to describe the relationship between grain size and the transition from low-to-high friction behavior in initially UNC materials. A critical grain size (~10nm) where plasticity changes from GB- to dislocation-mediated mechanisms was defined to predict the transition in friction behavior. In the case of initially coarse-grained metal, it was suggested that a combination of rapid initial grain refinement through plastic deformation and stress-driven grain growth drives the microstructure toward a value above or below a critical threshold where either dislocation (and high friction) or GB-mediated plasticity (and low friction) dominates [18]. This might suggest that the grain refinement of initially elongated NiCr grain structure in the case of passed and failed tests is associated with different plasticity mechanisms which give rise to different levels of wear.

The grain refinement results in an increase of the hardness of the near-surface material due to an increase of the density of grain boundaries and dislocation accumulation, but it also leads to a lower capacity of deformation, and therefore to brittleness [18-21].

Hence, the frictional shear experienced by the contact during endurance test promotes the release of wear nanoparticles from the embrittled near-surface of the NiCr track TTL. These wear particles may easily be embedded in the softer AgPd cursor and TEM investigations indeed give evidence that they may ultimately form a thick and adhesive third body on the surface of AgPd cursor. This third body is found to have a nanocrystalline structure, maybe further refined during the harsh event of detachment and adhesion. More importantly, it is deprived of its chromium (see Section 6.2). The NiCr track hardness has been estimated at 3 GPa [14] with the initial grain structure. It is probably still harder once refined into a nanocrystalline layer during the initial, mild wear stages of the contact. The selectivity of the transfer is maybe important here to explain the severe wear of the contact. Popov et al. [11] have shown that Ni surface of 1.5 GPa hardness once work hardened superficially under severe friction is subjected to a grain refinement which leads to a nanocrystalline TTS and an increase of its hardness to ~5 to 6 GPa in the first micrometers below the surface. In the present work, the hardness of the 500 nm third body could not be measured but the structure of this Ni nanolayer, very similar in size or even finer than in Popov et al.'s study [11], suggests a hardness of the same level. This might be sufficient to promote the severe wear of NiCr evidenced [14], even with its refined structure. The formation of the third body on the AgPd surface could thus lead to a change of the characteristics of the contact from AgPd (H~1.5 GPa) - NiCr (H~3 GPa) to Ni (H~6 GPa) –NiCr (hardened to H~4-5 GPa).

Transfer events generally show some stochastic character, degenerating or not depending on hidden variables pertaining to micro-surface defects, temporary lubricant shortage etc. Here, passed tests are characterized by the fact that few if any of these wear particles are formed and that they either do not adhere to the cursor, or the few of them that do are readily worn off by subsequent sliding. Note that some quasi-pure Ni fragments detached from the third body have been observed back into the NiCr track (Figure 5), which supports the brittleness and/or moderate adhesion of the third body on AgPd.

On the contrary, severe wear ("failed tests") results from cumulative nanoparticle wear and adhesion events when the elimination mechanisms are overwhelmed by fast arrival of new particles due to an increase of the boundary character of the lubrication (local starvation e.g.).

6.2 Chemical composition of the adhesive transfer layer

TEM-EDS analyses have evidenced the selective character in Ni of the third body formed on the AgPd cursor.

While selective transfer in frictional contact was already reported in the literature particularly for copper alloys [22], to the best of our knowledge, this is the first time that the formation of Ni selective third body from NiCr surface is observed.

Kragelskii et al. [22] have shown the formation of selective transfer during frictional contact between copper-zinc alloys and steel under boundary lubrication. The process is based on selective corrosion of the wear particles once released from the surface. They suggested that their lubricant, glycerin, played the role of an electrolyte enhancing the selective dissolution of zinc, which gives rise to a third body rich in copper forming a low-friction, porous layer soaked with lubricant. Should anything similar occur here, wear particles released from the NiCr track would lose their Cr owing to the electronegativity difference between Cr (1.66) and Ni (1.91). However dissolution of chromium in a silicone oil is not probable.

More generally, several factors might favor a selective transfer in metal-metal frictional contacts such as the thermal instability of lubricant and/or of the friction pairs, severe contact conditions (pressure, sliding speed, contact temperature) or the catalytic effect of the metallic compounds over the lubricant. Phenomena such as the formation of double electric layer, the enhancement of the density of superficial dislocations, the destruction of oxide layers, the emission of electrons are found to be associated with process of selective transfer [23].

In the following, some tentative explanations are given to the disappearance of Cr, which could occur at any time between the releasing of worn particles from the NiCr track and their adhesion on the AgPd cursor followed by continued sliding.

It is worth pointing out that the NiCr material is a solid solution alloy composed of Ni:Cr ratio of 80:20. The near-surface of the NiCr track subjected to grain refinement has a similar chemical composition than the bulk NiCr. The absence of chromium was observed only in the third body on the cursor and in the corresponding detached fragments re-embedded into the NiCr track as shown in Figure 6 and 7.

Note that the contact was lubricated using chlorinated silicone oil, PTFE-thickened grease.

Several hypotheses could explain the disappearance of Cr in the third-body:

- The volatile character of some Cr^{VI} salts such as oxides, hydroxides, chlorides. It has been evidenced generally at temperatures above 600°C, e.g. in steelmaking of stainless steels (FeCr or FeCrNi alloys) or in Solid Oxide Fuel Cells (SOFC) [24-27]. But it has been found also between 150°C and 250°C by mass spectrometry of pure solid CrO_3 in a heated boron nitride Knudsen cell, showing congruent sublimation CrO_3 solid → CrO_3 gas, as studied by McDonald et al. [26] ;
- The catalytic effect of some compounds of the cursor such as Pd and Ag (and also a small amount of Cu). Kumara et al. [27] claim a synergistic catalytic effect on organic reactions when Ag and Pd nanoparticles are mixed with a lubricant. On the other hand, Cu oxide is claimed by Tabor and Willis. [28] to catalyse oxidative attack of the silicone chain as a first step of the tribopolymerization of silicone oils. The latter has also been observed by the present authors in another contact involving the same cursor [29]. All three major elements of the cursor can therefore be involved in catalytic activity towards the chlorine-containing silicone oil. In the current sensors, high temperatures have not been detected and due to mild conditions, macroscopic temperatures are not expected to rise very high. However, at the micro- and nano-

scale, the large plastic strain experienced by the NiCr surface necessarily dissipates a large density of energy which might result in quite high flash temperatures.

It is therefore speculated that during the running-in phase of the endurance tests, as wear nanoparticles of both NiCr and AgPd are detached and mixed with the lubricant in the interfacial medium, some reactions may take place involving oxygen and maybe chlorine from the silicone oil, resulting in evaporation of Cr salts from the NiCr nanoparticles, leaving quasi-pure Ni.
These reactions seem to take place only once the wear nanoparticles are delivered into the contact probably due to their large surface / volume ratio and not on the deformed near-surface of the track where the Ni:Cr ratio remains nominal.
It must be noted that additional endurance tests (not shown here) have been conducted with AuPt cursors, with slightly different contact parameters. They have given the formation of a third body selective in Ni, which could be explained by a possible catalytic effect of platinum. On the contrary, friction tests carried out on a pin-on-disk tribometer using a steel pin on the NiCr surface did not give rise to a selective third body despite the formation of wear particles and the presence of the same lubricant. These results support the hypothesis of possible catalytic effects of the cursor elements. However further investigations would be necessary to determine the chemical mechanisms behind the disappearance of chromium (Cr) from the third body.

6.3 Ability of Alumina to protect the contact against adhesive transfer

The tumble finishing treatment using alumina powder has a beneficial impact on the NiCr tracks by smoothing their surfaces and deburring their edges. Hence, it contributes to limit direct contact between sharp asperities.
At the same time, this treatment is expected to have a moderate effect on the refinement of NiCr microstructure, which leads to only a slight increase of the top surface hardness. This increase of hardness contributes to limit the generation of wear nanoparticles from the NiCr surface during the running-in period of the endurance tests, which is believed to be the primary cause of the third body formation. Moreover, the adhesion of alumina powder on the surface of the NiCr tracks contributes to preserve the surfaces from direct contact with the cursor and therefore, from severe wear (Figure 11).
In addition, several papers have pointed out the effectiveness of alumina powder with lamellar structure as an anti-wear additive in lubricants [30-32]. TEM images of the treated NiCr track have revealed the removal of alumina from the NiCr surface after an endurance test. This suggests that the alumina powder present on the NiCr surface and in the valleys of the track was continuously mixed with the grease during the cyclic movements of the cursor, playing the role of an anti-wear, solid lubricant additive.
The addition of an anti-wear additive in grease is known to improve its efficiency especially in the boundary lubrication regime by preventing direct asperity contact through the formation of a thin boundary film.
As shown in Figure 15, chemical mapping made on the cross-section of the treated NiCr track revealed the presence of a very thin transfer layer composed mainly of Ag and Pd elements. The increase of the wear resistance of the NiCr surface induced by the tumble finishing treatment is found to favor the wear of the softer AgPd surface which gives rise to the formation of a transfer layer on the NiCr surface. However, the wear rate of AgPd surface is moderate as shown by the low thickness of the transfer layer. AgPd wear nanoparticles were probably generated since the first cycles of the endurance test, resulting in flattening the contact area of the curved cursor as shown in [14]. This mild wear of AgPd cursor contributes to enlarge the electric contact surface which improves the contact conductance.

It must be noted that alumina has not systematically avoided any Ni-rich transfer film on the cursor. Indeed such films have been found during running-in or early stages of endurance tests. In this case, traces of Cr remained however, contrary to previous findings. These transfer layers disappeared systematically later on. This points to the effect of contact conditions on the balance between adherence of new particles and detachment of elements from the transfer film [15,16]: milder contact due to solid lubrication by alumina has displaced the equilibrium point. The residual chromium proves that in this case, Cr elimination has not come to completion: flash temperature may have been lower, or the duration of these interrupted tests may not have been sufficient for this. Perhaps less refined grains lead to bigger wear particles from which not all chromium could be extracted.

The main cause of the deterioration of the endurance life of sensors is the formation of hard nanostructured third body in the contact. Using alumina in the tumble finishing treatment has thus proved to be a good solution to prevent the damage of contact surface and to maintain stable and low electrical resistance of sensors. Alumina powder acts as a 'solid lubricant' in improving friction and limiting adhesion of wear nanoparticles on both AgPd and NiCr surfaces.

7. Conclusion

This work has investigated the tribological behavior, wear and adhesive transfer, of AgPd-NiCr electrical contact in order to improve the endurance lifetime of electrical compounds. Endurance tests show that in spite of the mild loading conditions experienced by the contact (low nominal contact pressure ~5 MPa) and the use of a grease as a lubricant, the cyclic sliding movements induce a SPD of the NiCr track surface and the formation of an adhered third body on the AgPd cursor surface [14]. The analyses of the present paper have shed some light on the mechanisms:

- TEM analyses reveal the nanostructured character of the third body and its selectivity in Ni, which both contribute to change the nature of the initial contact from AgPd-NiCr to nano-Ni-NiCr. This third body has a severe abrasive action on the NiCr surface due to its high hardness, resulting in a typical measured wear loss of 10% of the total thickness of the conducting track and significant deterioration of the electrical response of sensors;
- Catalytic effects of elements present in the cursor such as Pd, Ag (and Cu), possibly in interaction with the chlorine-containing silicone oil, are proposed to explain the absence of Cr in the adhered third body. However, further investigations are needed to confirm this;
- Alumina-assisted tumble finishing was introduced in order to repair NiCr surface heterogeneities especially at the edges of the tracks. Besides the edge deburring and surface smoothing actions, alumina powder was found to cover most of the NiCr surface. Its solid lubricant action avoids in the end adherent nano-Ni film formation on the cursor and the resulting severe wear of the track. During the endurance tests, alumina covering the NiCr surface and filling the valleys may also be mixed to the grease, forming a solid additive improving the efficiency of the grease in terms of wear protection.The synergetic combination of all these effects has led to avoid severe wear of the NiCr track. The formation of an abrasive third body was stopped as evidenced by TEM analyses. In addition, TEM investigations have revealed the presence of a very thin, softer transfer in the other direction, from the AgPd cursor to the NiCr track. This transfer both protects NiCr against wear and improves the conductivity of the contact. Thus, by displacing the equilibrium points of the formation and elimination mechanisms of track-to-cursor and cursor-to-track transfers, tumble

finishing associated with alumina powder preserves surfaces from severe wear and increases the electrical lifetime of the sensors.

Acknowledgement

The authors gratefully acknowledge financial support from ANRT (CIFRE grant nr 1262/2016).

The authors wish to thank Philippe Vennéguès for his help with TEM analyses, the Direction of IMRA Europe for permitting us to access the TEM, and Suzanne Jacomet for her assistance with the SEM analyses.

References

[1] S. Jacobson, S. Hogmark, "Surface modifications in tribological contacts", *Wear*, vol. 266, pp. 370-378, 2009.

[2] M. Godet, "The third-body approach : a mechanical view of wear," *Wear*, vol. 100, pp. 437–152, 1984

[3] Y. Estrin, and A. Vinogradov, "Extreme grain refinement by severe plastic deformation: A wealth of challenging science", *Acta Mater.*, vol.61, pp. 782-817, 2013.

[4] V. M. Segal, "Materials processing by simple shear", *Mater.Sci. Eng.*, vol. A197, pp.157-164, 1995.

[5] S. Descartes, C. Desrayaud, and E. F. Rauch, "Inhomogeneous microstructural evolution of pure iron during high-pressure torsion", *Mater. Sci. Eng.*, vol. A528, pp. 3666-3675, 2011.

[6] Z. Yanushkevich, A. Belyakov, R. Keibyshev, C. Haase, and D.A. Molodov, "Effect of cold rolling on recrystallization and tensile behavior of a high-Mn steel", *Mater. Charact.*, vol. 112, pp. 180-187, 2016.

[7] Y.Saito, H. Utsunomiya, N. Tsuji, and T. Sakai, "Novel ultra-high straining process for bulk materials-development of the accumulative roll-bonding (ARB) process", *Acta Mater.*, vol. 47, no. 2, pp. 579-583, 1999.

[8] J. Marteau and S. Bouvier, "Characterization of the microstructure evolution and subsurface hardness of graded stainless steel produced by different mechanical or thermomechanical surface treatments", *Surf. Coat. Technol.*, vol. 296, pp. 136-148, 2016.

[9] S. Q. Deng, A. Godfrey, W. Liu, and N. Hansen, "A gradient nanostructure generated in pure copper by platen friction sliding deformation", *Scr. Mater.*, vol. 117, pp. 41-45, 2016.

[10] A. Moshkovich, I. Lapsker, Y. Feldman, L. Rapoport, "Severe plastic deformation of four FCC metals during friction under lubricated conditions", *Wear*, vo. 386-387, pp. 49-57, 2017.

[11] I. Popov, A. Moshkovich, S. R. Cohen, V. Perfilyev, A. Vakahy, and L. Rapoport, "Microstructure and nanohardness of Ag and Ni under friction in boundary lubrication," *Wear*, vol. 404–405, pp. 62–70, 2018.

[12] N. Saka, M. J. Liou, and N. P. Suh, "The role of tribology in electrical contact phenomena," *Wear*, vol. 100, pp. 77–105, 1984.

[13] M. Antler, "Wear, friction and electrical noise phenomena in severe sliding systems," *ASLE Trans*, vol. 5, no. 2, pp. 297–307, 1962.

[14] M. Isard, I. Lahouij, P. Montmitonnet, and J.-M. Lanot, "Third-body formation by selective transfer in a NiCr/AgPd electrical contact. Consequences on wear and remediation by a barrel tumble finishing," *Wear*, vol. 426–427 B, pp. 1056–1064, 2019.

[15] P. Montmitonnet, F. Delamare, B. Rizoulières : Transfer layer and friction in cold metal strip rolling processes. Wear 245, pp. 125-135, 2000.

[16] P. Montmitonnet, E. Felder: A Third-Body Modelling Strategy for the Prediction of Adhesive Transfer Layer Formation on Forming Tools. Proc. ICTMP 2016 (Phuket, Thailand, 29 Feb – 2 March 2016), Thai Tribology Association, pp. 62-73, 2016.

[17] F. Salvatore, F. Grange, R. Kaminski, C. Claudin, G. Kermouche, J. Rech, A. Texier, "Experimental and numerical study of media action during tribofinishing in the case of SLM titanium parts," *Procedia CIRP*, vol. 58, pp. 451 – 456, 2017.

[18] N. Argibay, T.A. Furnish, B.L. Boyce, B.G. Clark, M. Chandross, "Stress-dependent grain size evolution of nanocrystalline Ni-Wand its impact on friction behavior", Scripta Mat. 123 (2016) pp. 26–29

[19] E. Frutos, M. Multigner, and J. L. Gonzalez-Carrasco, "Novel approaches to determining residual stresses by ultramicroindentation techniques: Application to sandblasted austenitic stainless steel," *Acta Mater.*, vol. 58, pp. 4191–4198, 2010.

[20] C. Rynio, H. Hattendorf, J. Klower, G. Eggeler, "On the physical nature of tribolayers and wear debris after sliding wear in a superalloy/steel tribosystem at 25 and 300 °C", *Wear*, vol. 317, pp. 26-38, 2014.

[21] A. Dreano, S. Fouvry, G. Guillonneau, "A tribo-oxidation abrasive wear model to quantify the wear rate of a cobalt-based alloy subjected to fretting in low-to-medium temperature conditions", *Tribology International*, vo. 125, pp. 128-140, 2018.

[22] I.V. Kragelskii, N.M. Mikhin, N.K. Myshkin, M.A. Bronovets, M.N. Dobychin, V.N. Dubnyakov, V.N. Litvinov, “The mechanism of the initial stage of selective transfer during frictional contact”, Wear 47 pp.133-138, (1978).

[23] C Kajdas, K Hiratsuka, “Tribochemistry, tribocatalysis, and the negative-ion-radical action mechanism”, Proc. IMechE Vol. 223 Part J: J. Engineering Tribology, pp 827-848, 2009.

[24] R. Sachitanand, M. Sattari, J. -E. Svensson, and J. Froitzheim, "Evaluation of the oxidation and Cr evaporation properties of selected FeCr alloys used as SOFC interconnects", *Int. J. Hydrogen Energy*, vol. 38, pp. 15328-15334, 2013.

[25] S. Seetharaman, G. J. Albertsson, and P. Scheller, "Studies of vaporization of chromium from thin slag films at steelmaking temperatures in oxidizing atmosphere", *Metall. Mater. Trans.*, vol. 44B, pp. 1280-1286, 2013.

[26] H. Falk-Windisch, M. Sattari, J. -E. Svensson, and J. Froitzheim, "Chromium vaporization from mechanically deformed pre-coated interconnects in solid oxide fuel cells", *J. Power Souces*, vol. 297, pp. 217-223, 2015.

[27] C. Collins, J. Lucas, T. L. Buchanan, M. Kopczyk, A. Kayani, P. E. Gannon, M. C. Deibert, R. J. Smith, D. -S. Choi, V. I. Gorokhovsky, "Chromium volatility of coated and uncoated steel interconnects for SOFCs", S*urf. Coat. Technol.*, vol. 201, pp. 4467-4470, 2006.

[28] J.D. McDonald and J.L. Margrave, “Mass spectrometric studies at high temparatures. Sublimation and vaporization of chromium trioxide”, *J. inorg. Nucl. Chem.*, vol. 30, pp. 665-667, 1968.

[29] C. Kumara, H. M. Meyer III, and J. Qu, “Synergistic interactions between silver and palladium nanoparticles in lubrication”, *ACS Appl. Nano Mater.*, vol. 2, no. 8, pp. 5302-5309, 2019.

[30] D. Tabor and R. F. Willis, “The formation of silicone polymer films on metal surfaces at high temperatures and their boundary lubricating properties,” Wear, vol. 13, pp. 413–442, 1969.

[31] M. Isard, I. Lahouij, P. Montmitonnet, and J.-M. Lanot, “Troisième corps adhérent dans un contact polymère – métal lubrifié par une graisse silicone : exemple de tribo-polymérisation ?” (Adherent 3rd body in a polymer-metal contact lubricated by a silicone-based grease : an example of tribopolymerization ?), *JIFT 2019 (Tours, France, 24 – 26 April 2019)*. In French.

[32] D. Jiao, S. Zheng, Y. Wang, R. Guan, and B. Cao, “The tribology properties of alumina / silica composite nanoparticles as lubricant additives”, *Appl. Surf. Sci.*, vol. 257, pp. 5720 – 5725, 2011.

[33] M. K. A. Ali, A. Elagouz, and M. A. A. Abdelkareem, “Minimizing of the boundary friction coefficient in automotive engines using Al2O3 and TiO2 nanoparticles”, *J. Nanoparticle Res.*, vol. 18:377, pp. 1 – 16, 2016.

[34] L. Pena-Paras, J. Taha-Tijerina, and L. Garza, “Effect of CuO and Al2O3 nanoparticle additives on the tribological behavior of fully formulated oils”, *Wear*, vol 332 – 333, pp. 1256-1261, 2015.